JHC

Melatonin Ameliorates Injury and Specific Responses of Ischemic Striatal Neurons in Rats

Yuxin Ma[1], Qiqi Feng[1], Jing Ma, Zhibo Feng, Mali Zhan, Lisi OuYang, Shuhua Mu, Bingbing Liu, Zhuyi Jiang, Yu Jia, Youlan Li, and Wanlong Lei

Department of Anatomy, Zhongshan School of Medicine, Sun Yat-sen University, Guangzhou, People's Republic of China (YM, QF, MZ, LOY, SM, BL, ZJ, YJ, YL, WL); Department of Anatomy, School of Basic Medicine, Guangdong Pharmaceutical University, Guangzhou, People's Republic of China (YM); Health Center, Xintang Hospital, Zengcheng, Guangzhou, People's Republic of China (JM); and Department of Anatomy, Xinxiang Medical University, Xinxiang, People's Republic of China (ZF).

Summary

Studies have confirmed that middle cerebral artery occlusion (MCAO) causes striatal injury in which oxidative stress is involved in the pathological mechanism. Increasing evidence suggests that melatonin may have a neuroprotective effect on cerebral ischemic damage. This study aimed to examine the morphological changes of different striatal neuron types and the effect of melatonin on striatal injury by MCAO. The results showed that MCAO induced striatum-related dysfunctions of locomotion, coordination, and cognition, which were remarkably relieved with melatonin treatment. MCAO induced severe striatal neuronal apoptosis and loss, which was significantly decreased with melatonin treatment. Within the outer zone of the infarct, the number of Darpp-32+ projection neurons and the densities of dopamine-receptor-1 (D1)+ and dopamine-receptor-2 (D2)+ fibers were reduced; however, both parvalbumin (Parv)+ and choline acetyltransferase (ChAT)+ interneurons were not significantly decreased in number, and neuropeptide Y (NPY)+ and calretinin (Cr)+ interneurons were even increased. With melatonin treatment, the loss of projection neurons and characteristic responses of interneurons were notably attenuated. The present study demonstrates that the projection neurons are rather vulnerable to ischemic damage, whereas the interneurons display resistance and even hyperplasia against injury. In addition, melatonin alleviates striatal dysfunction, neuronal loss, and morphological transformation of interneurons resulting from cerebral ischemia. (J Histochem Cytochem 61:591–605, 2013)

Stroke, mostly ischemic, is the second most common cause of death and major cause of disability worldwide (Donnan et al. 2008). Focal cerebral ischemia leads to transient or permanent interruption of blood flow in specific brain structures, consequently causing specific brain damage and functional disruptions, with the striatum as one of the main targets (Block et al. 2005; Reiter et al. 2005). To further investigate the underlying mechanisms, middle cerebral artery occlusion (MCAO) has been utilized to induce cerebral ischemia in animals (Yamori et al. 1976). Previous studies show that MCAO causes motor and cognitive dysfunctions as well as histological injuries in the striatum in

experimental animals (Carmichael 2005; Liu et al. 2009). Nevertheless, the characteristic responses and morphological changes of different striatal neuron types resulting from ischemic insult have not yet been elucidated.

Corresponding Author:
Wanlong Lei, Department of Anatomy, Zhongshan School of Medicine, Sun Yat-sen University, 74 Zhongshan Rd 2, Guangzhou 510080, China.
E-mail: leiwl@mail.sysu.edu.cn; wllei2001@yahoo.com

The striatum is a heterogeneous subcortical structure in terms of its neuronal types, which include projection neurons (accounting for 90–95% of striatal neurons in rodents) and interneurons (constituting 5–10% in rodents) (Durieux et al. 2011). Interestingly, studies suggested that different types of striatal neurons exhibited distinctive susceptibility to various forms of brain damage, including cerebral ischemia: the projection neurons were rather vulnerable to injury, whereas the striatal interneurons generally survived in the ischemic core and the penumbra, which is considered as a therapeutic target in cerebral ischemia (Meade et al. 2000; Larsson et al. 2001; Pestalozza et al. 2002). Several studies have shown that various interneuron types, such as the choline acetyltransferase (ChAT)+ and neuropeptide Y (NPY)+ neurons, were spared after ischemic damage (Meade et al. 2000; Larsson et al. 2001). Yang et al. (2008) even found neurogenesis of calretinin (Cr)+ striatal interneurons induced by hypoxia/ischemia in neonatal rats. The resistance of striatal interneurons was also reported in a model of Huntington's disease (HD) induced by 3-nitropropionic acid (3NP) or quinolinic acid (QA) (Cicchetti et al. 1996; Figueredo-Cardenas et al. 1998; Mu et al. 2011b). Taken together, these studies suggest that striatal interneurons may possess unique abilities against injury factors (Meade et al. 2000) and different interneuron types may be subjected to distinct pathophysiological processes.

Melatonin, a bioactive compound secreted primarily by the pineal gland in mammals, possesses a variety of physiological functions including regulating circadian and seasonal rhythms (Quay 1989), removing free radicals, and preventing oxidation of biomolecules (Maldonado et al. 2007; Tan et al. 2007). Earlier research has revealed that a reduction in melatonin is related to various degenerative diseases such as Alzheimer's disease, HD, and Parkinsonism, and thus this compound has been tested for treating various neurodegenerative disorders (Reiter et al. 1999; Srinivasan et al. 2005). Lately, increasing evidence demonstrates that melatonin has neuroprotective effects against transient or permanent ischemic brain injury (Pei et al. 2002a; Kilic et al. 2004a; Nair et al. 2011). Its protective effects are believed to stem from direct free radical scavenging and indirect antioxidant activities possibly at the mitochondrial level (Reiter et al. 2005). Koh (2008, 2012) further reported that melatonin protected against cerebral ischemia by disrupting the apoptotic cascades and attenuating glutamate toxicity in neurons using rat models. Altogether, these studies suggest that melatonin may be a novel therapeutic agent for ischemic stroke.

To test our hypothesis, a rat model of MCAO was used to detect the behavioral and histological changes in the present study, providing a more comprehensive and profound understanding of the specific morphological changes of different striatal neuron types after MCAO. Furthermore, the protective effect of melatonin on different types of striatal neurons after ischemic damage was also verified.

Materials and Methods

Experimental Animals and Melatonin Treatment

Thirty-six adult male Sprague-Dawley (SD) rats weighing 300–350 g (obtained from the Center for Experimental Animals of Sun Yat-sen University) were used in this study. The animals were housed in a room under an even dark/light cycle and had free access to water and a standard rat diet. All animal experiments strictly adhered to the Regulations for the Administration of Affairs Concerning Experimental Animals, the Chinese national guideline for animal experiment, issued in 1988. All procedures involving animals and their care in this study were approved by the Animal Care and Use Committee of Sun Yat-sen University (Permit Number: SCXK GUANGDONG 2011–0029). The rats were randomly divided into five groups: normal (n=6), control (or sham-operated, n=6), MCAO (n=8), MCAO+vehicle (n=8), and MCAO+MT (MT short for melatonin, n=8).

Melatonin (Sigma-Aldrich, St. Louis, MO) was dissolved in saline containing less than 5% ethanol. A single dose of melatonin was given at 10 mg/kg via intraperitoneal injection to the MCAO+MT group 30 min before the onset of the MCAO procedure. The MCAO+vehicle group received saline only.

Middle Cerebral Artery Occlusion Procedure

The rats in the MCAO, MCAO+vehicle, and MCAO+MT groups underwent permanent MCAO procedures, as described previously (Nishino et al. 1993). The animals were anesthetized with ketamine (150 mg/kg) and incised medially in the neck using blunt dissection techniques. The right common, external, and internal carotid arteries were exposed and isolated carefully from the vagus nerve. After clamping the common and internal carotid artery, the external carotid artery was tied and a small hole was made in its branch. A monofilament was inserted through the hole and advanced to a length of 18–20 mm via the internal carotid, finally reaching the middle cerebral artery (MCA). Then the incision was sutured. The rats in the control group received the same procedures, except that the MCA was not occluded.

Behavioral Tests

Behavioral tests were carried out on the third day after the surgery. Examiners were blinded to animal conditions.

Balance Beam Test. All rats were tested using a balance beam three times a day for five consecutive days according to Shear's methods (Shear et al. 1998). The rats were trained to travel across a suspended narrow beam (100 cm in length, 7 cm in width, 100 cm elevated above the horizontal surface of the ground) into a dark box (24.5 × 20 × 18 cm) at the other end. The latency of initiating movement (the interval

between the moment the rat was placed on the start point of the beam and the point it moved 20 cm forward), completion time (the interval between the moment the rat reached the 20 cm point to the moment it entered the dark box), and the number of foot slips (the forelimb descending more than 1.5 cm below the surface of the beam) were recorded by two observers. Animals were given 3 min to complete a trial. If the rat fell down or took more than 3 min, this trial was recorded as incomplete.

Grip Strength Test. Grip strength (Shear et al. 1998) was measured by recording the length of time the rat was able to hold on a steel wire (2 mm in diameter, 35 mm in length) suspended 50 cm above the horizontal surface of the ground. Grip strength was measured three times a day for five consecutive days.

Morris Water Maze Task. In the Morris water maze task (Packard and Knowlton 2002; Vorhees and Williams 2006), all rats were trained four times a day for five consecutive days, followed by the probe trial on the last day. The target platform was located in different spatial locations across trials, but the visual pattern of the ball which served as a cue was consistent. During each trial, rats were released from four assigned starting points (N, S, E, W) and allowed to swim for 2 min. The rats were allowed to stay on the platform for 30 sec once they reached the platform or if they failed within 2 min. In the probe trial, the platform was removed from the tank. The tracks were recorded by a camera and Ethovision software (Noldus, Holland). This task could be acquired by learning an approach response to the visual cue, which was believed to be associated with the mnemonic functions of the striatum.

Histochemical and Immunohistochemical Staining

After the five-day behavioral tests, all rats were sacrificed for histological examinations. Before the following procedures, animals were deeply anesthetized with 10% chloral hydrate (350 mg/kg).

TTC Staining. The brains were rapidly removed and each forebrain was sectioned coronally into five slices (1.5-mm thick), then stained with 2% 2, 3, 5-triphenyltetrazolium chloride (TTC) at 37C for 30 min, and transferred to 4% paraformaldehyde for postfixation.

HE and Nissl Staining. Animals were perfused with 0.9% saline followed by 4% paraformaldehyde in 0.1 M phosphate buffer (pH 7.4, 4C). Brains were removed and postfixed overnight at 4C. Sections (50-μm) were cut using a vibratome and stained with hematoxylin and eosin (HE) and Nissl staining according to previous classic methods (Voogd and Feirabend 1981; Mu et al. 2011a).

Immunohistochemistry Procedures. All rats were perfused with 0.9% saline followed by 4% paraformaldehyde in 0.1 M phosphate buffer (pH 7.4, 4C). Brains were removed and postfixed overnight at 4C, and then cut into sections (50-μm thick) using a vibratome. Brain sections were treated with 0.3% H_2O_2 in 0.01 M phosphate buffered saline (PBS, pH 7.4) at 4C for 30 min, and then were incubated at 4C for 36–40 hrs with one of the following primary antibodies (details of the antibodies are listed in Table 1): anti-NeuN, anti-Darpp-32, antidopamine receptor 1 (anti-D1), antidopamine receptor 2 (anti-D2), anti-NPY, anti-Cr, anti-Parv, or anti-ChAT. Sections were rinsed and incubated in anti-mouse IgG, anti-rabbit IgG or anti-rat IgG (1:200, Sigma) for 3 hrs, followed by incubation in homologous peroxidase-antiperoxidase (PAP) complex (1:200, Sigma) at room temperature for 2 hrs. The peroxidase reaction was performed using 3, 3'-diaminobenzidine (DAB, 0.05% in 0.01 M PB, pH 7.4, Sigma) for 2–10 min. Between each procedure, sections were repeatedly rinsed three times in 0.01 M PBS for 5 min.

TUNEL Assay. To examine whether striatal neurons underwent apoptosis following MCAO, TUNEL assay was performed using an in situ cell death detection kit (POD, Roche). Sections (50-μm thick) were subjected to TUNEL labeling according to the manufacturer's instructions.

Data Collection and Statistical Analysis

Measurement of Infarcted Volume. TTC-stained brain sections (1.5-mm thick, five for each brain) were photographed using a digital camera, and then the infarcted areas of the striatum were recorded as images and quantified using Image-Pro Plus 6.0 software (Media Cybernetics, Bethesda, MA). The infarcted volume was calculated by multiplying the infarcted areas with the thickness of each section, as previously described (Hyakkoku et al. 2009; Yang et al. 2011). To acquire more precise data, an unbiased estimator of volume based on the Cavalieri principle was used to measure the infarcted volumes in the HE- and Nissl-stained sections (50-μm thick) (Avendano et al. 1995; Matsumori et al. 2006). The measurement was carried out on every 11th section of the brain containing the striatum (2.5 mm anterior and 3.3 mm posterior to bregma, 10 to 11 sections per animal for each staining method). The infarcted areas of the striatum were recorded by a digital camera and quantified using Image-Pro Plus 6.0 software. The infarcted volume was calculated by integration of all the infarcted areas and the distance between them.

Quantification of Neuron Number and Process Density. The outer zone of the infarct in the striatum, the narrow girdle-shaped zone of lesser neuron loss surrounding the ischemic lesion core (Mu et al. 2011c), was the focus in the present

Table 1. Antibody information.

Antibody	Type and Host	Source	Catalog Number	Antigen	Dilution Used
Neuron-specific nuclear protein (NeuN)	Mouse monoclonal	Millipore/ Chemicon	MAB377	Purified cell nuclei from mouse brain	1:1000
Dopamine and cyclic AMP-regulated Phosphoprotein (Darpp-32)	Rabbit monoclonal	Cell Signaling	2302	Synthetic peptide corresponding to residues surrounding Thr34 of human Darpp-32	1:200
Dopamine D1 receptor	Rat monoclonal	Sigma-Aldrich	D187	C-terminal 97 amino acids of the human dopamine D1 receptor	1:400
Dopamine D2 receptor	Rabbit polyclonal	Millipore/ Chemicon	AB5084P	A 28 amino acid peptide sequence from the human dopamine D2 receptor within the cytoplasm	1:200
Neuropeptide Y (NPY)	Rabbit polyclonal	Abcam	Ab10980	Full length neuropeptide Y conjugated to KLH	1:500
Calretinin (Cr)	Rabbit polyclonal	Millipore/ Chemicon	AB5054	Recombinant rat calretinin	1:2000
Parvalbumin (Parv)	Mouse monoclonal	Sigma-Aldrich	P3088	Frog muscle parvalbumin	1:1000
Choline acetyltransferase (ChAT)	Rabbit polyclonal	Millipore/ Chemicon	AB143	Human placental enzyme	1:1000

study, and thus all quantifications of neuron numbers and process densities was performed within this region (0.38 ± 0.09 mm in width). The investigators were blinded to these different experimental treatment groups when conducting the measurements. The quantification was carried out on every 11th section of the brain containing the infarcted region in the striatum (2.5 mm anterior and 3.3 mm posterior to bregma, 10 to 11 sections per animal for each staining method) and the number of neurons and processes were counted throughout the depth of the section. The cell count was performed in the HE-, Nissl- and all immunohistochemical stained sections. Each sampled section was first viewed at 100× magnification using a light microscope (Olympus BHS, Tokyo, Japan) with a reticule (0.1 mm × 0.1 mm) in one eyepiece to observe the whole area of the outer zone of the infarct. This annular region was roughly divided into five even parts, and the reticule was moved into each part to count the neuron number within the reticule field at 400× magnification. The final neuron number of each staining method was the average of the numbers acquired from the 10 to 11 equidistantly sampled sections. The quantification of process density was performed in the NPY- and Cr-stained brain sections. In each sampled section, the density of axons was measured within five nonoverlapping areas sampled in the outer zone of the infarct (the sampling method was the same as that of the cell count), and the numbers of intersecting processes along a 100-µm length were counted and averaged as the process density. The final process density of each staining method

was the average of the numbers acquired from the 10 to 11 equidistantly sampled sections.

Statistical Analysis. All experimental data are presented as mean ± standard deviation. The statistical analyses of data were performed by Student's *t*-test or one-way ANOVA with SPSS 16.0 software (Chicago, IL) and $p<0.05$ was considered to be significant.

Results

During the experimental period, one rat died in the MCAO group (the mortality being 12.5% for the MCAO model), one died in the MCAO+vehicle group, and none in the other groups. For all other rats, there was no significant difference in weight among groups (data not shown). Statistical analyses were made between the normal and control (or sham-operated) groups as well as between the MCAO and MCAO+vehicle groups respectively, and there was no significant difference in behavioral tests and histological examination results (data not shown). Therefore, we provide data and statistical analyses only of the control, MCAO, and MCAO+MT groups in the following text.

Effects of Melatonin on Behavioral Changes of the Experimental Rats

In the balance beam test, MCAO rats had difficulty in passing across the beam, with body rigidity and paw slipping
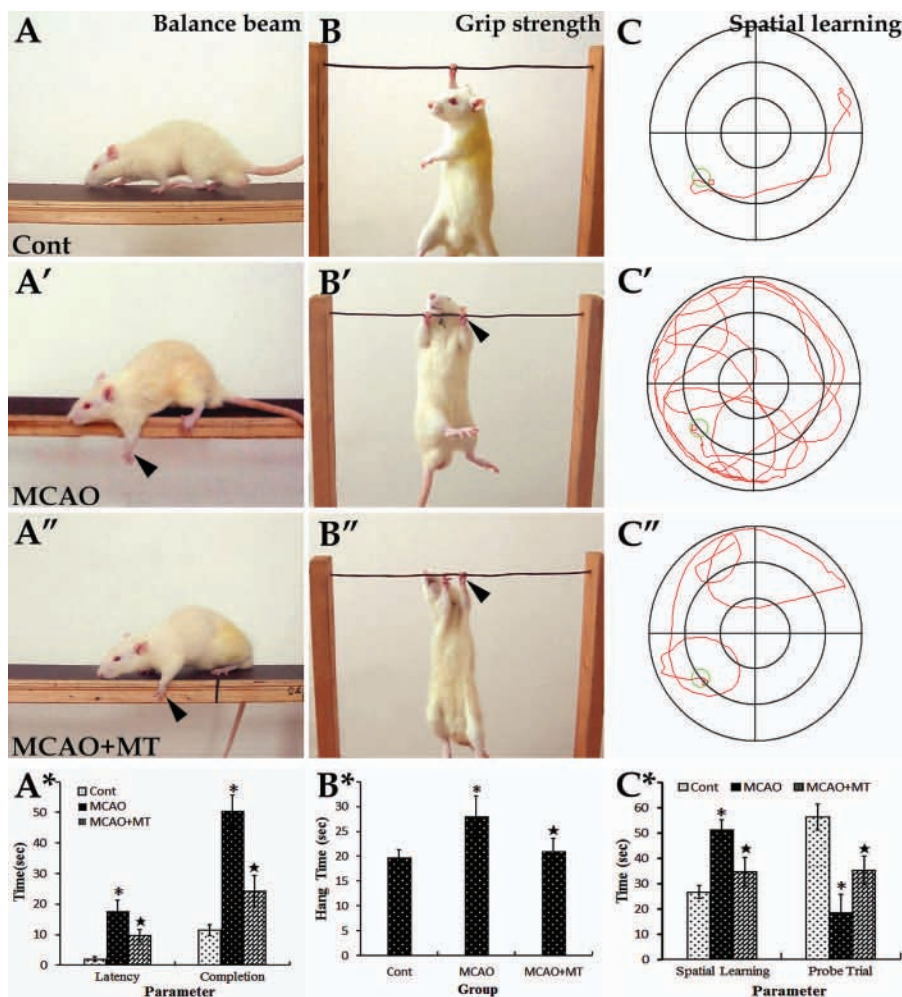
Figure 1. Behavioral changes of MCAO rats with melatonin treatment. In the balance beam test (image set A), the control rats were able to travel through the beam easily (A), whereas rats in the MCAO (A') and MCAO+MT (A") groups had difficulty in passing through the beam, with paw slipping observed (arrowheads). The latency of initiating movement and the completion time were both significantly decreased in the MCAO+MT group when compared with the MCAO group (A*). In the grip strength test (image set B), rats in the MCAO (B') and MCAO+MT (B") groups grasped the steel wire with obvious limb rigidity. The hang time in the MCAO+MT group was significantly decreased in comparison with the MCAO group (B*). In the Morris water maze task (image set C), the escape latency in spatial learning trials was notably increased and the time spent in target quadrant in the probe trial was reduced in the MCAO groups (C') in comparison to controls (C), but they were obviously improved in MCAO+MT rats (C" and C*). *$p<0.05$ MCAO vs. Cont (control, or sham-operated); ★$p<0.05$ MCAO+MT vs. MCAO.

observed (Fig. 1A'). The latency of initiating movement (17.80 ± 3.50 vs. control 2.00 ± 0.70, $p<0.05$) and completion time (50.50 ± 5.21 vs. control 11.50 ± 1.87, $p<0.05$) as well as the number of foot slips (3.39 ± 0.07 vs. control 0.08 ± 0.03, $p<0.05$) were all significantly increased in comparison with controls (Fig. 1A*). With melatonin treatment, the time to initiating movement (9.60 ± 2.07, $p<0.05$) and completing trials (24.17 ± 5.13, $p<0.05$) were both decreased when compared with the MCAO group (Fig. 1A" and A*). The number of foot slips was also improved (2.01 ± 0.06, $p<0.05$) in comparison with MCAO animals.

In the grip strength test, MCAO rats grasped the steel wire with obvious limb rigidity (Fig. 1B'), and the hang time (28.00 ± 4.13) was significantly increased when compared with controls (19.80 ± 1.47, $p<0.05$; Fig. 1B*). However, this increase in hang time was shorter and body rigidity was relieved after melatonin treatment. Statistical analyses revealed that there was a significant difference in hang time between the MCAO+MT group (21.00 ± 2.62, $p<0.05$) and the MCAO group (Fig. 1B" and B*).

Cognitive and mnemonic deficits were detected by means of the Morris water maze task. In contrast to the control animals, MCAO rats swam in much more irregular and bending routes when locating the hidden platform and moved more along the wall of the maze (Fig. 1C and C'). In the spatial learning test, the latency of locating the platform (51.18 ± 4.20) was significantly increased when compared with controls (26.67 ± 2.60, $p<0.05$); in the probe trial, the time spent in the target quadrant (18.50 ± 7.27) was notably decreased in comparison with controls (56.35 ± 5.27, $p<0.05$; Fig. 1C*). With melatonin treatment, the latency of locating the platform (34.74 ± 5.60, $p<0.05$) and the time spent in target quadrant (35.33 ± 5.65, $p<0.05$) were both improved in comparison with the MCAO group (Fig. 1C" and C*).

Morphological Changes of Ischemic Striatum and the Protective Effects of Melatonin

TTC staining was applied to assess the infarcted size induced by MCAO in the present study. MCAO produced a
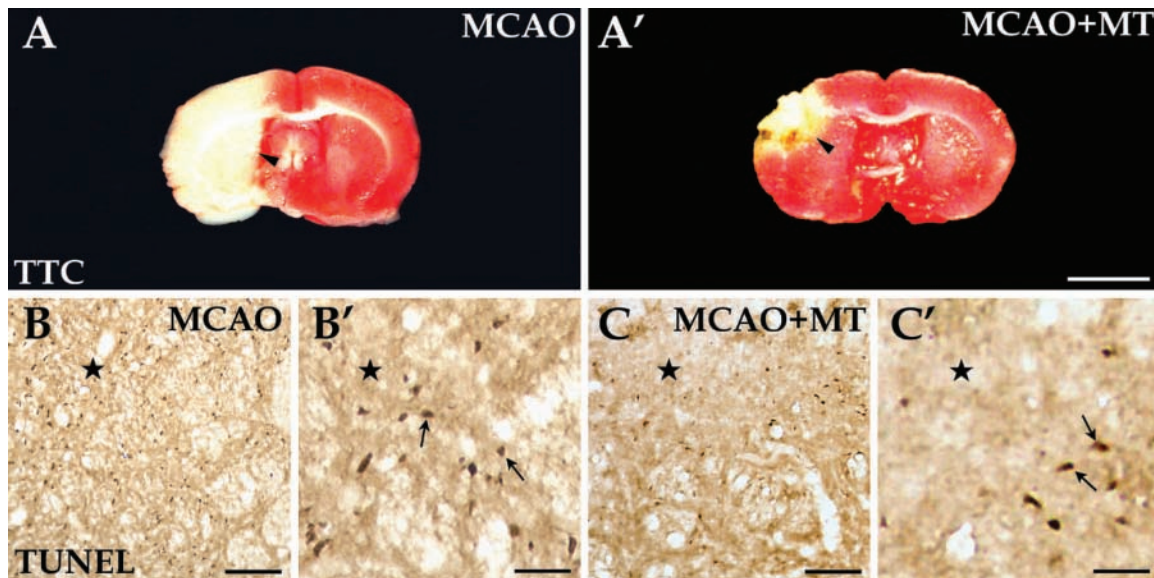
Figure 2. Improvements of ischemic area and in cellular apoptosis with melatonin treatment. TTC staining revealed that a large, pale ischemic area (arrowheads) was located in the striatum after MCAO (A), but it was obviously alleviated with melatonin treatment (A'). The TUNEL+ cells, or apoptotic cells (arrows), were present in large quantities in the ischemic region (★) of the MCAO group (B and B'), but were reduced in number in the MCAO+MT group (C and C'). Scale bars: A and A', 0.5 cm; B and C, 100 μm; B' and C', 30 μm.

clearly demarcated lesion located in the dorsolateral striatum and the infarcted damage broadly extended to the lateral and caudal cortex unilaterally (Fig. 2A). The infarcted area was less after melatonin was applied (Fig. 2A'). Statistical analyses revealed that the infarcted volume of the striatum in the MCAO+MT group (95.28 ± 5.45) was significantly smaller than that in the MCAO group (223.35 ± 23.62, $p<0.05$; Fig. 3A), which was also supported by Nissl (MCAO+MT 82.35 ± 9.10 vs. MCAO 248.26 ± 16.37, $p<0.05$) and HE staining (MCAO+MT 78.55 ± 9.12 vs. MCAO 203.47 ± 14.50, $p<0.05$; Fig. 3A; Fig. 4).

Histological changes to the injured striatum were assessed using Nissl and HE staining. TUNEL assay was also used to detect the degree of neuronal apoptosis in the striatal infarcted area. In general, the infarcted area consisted of the ischemic core with dark staining and the outer zone of light staining closely surrounding the ischemic core (Fig. 4A and C). In the dense ischemic core, where a large quantity of inflammatory cells infiltrated, very few neurons survived (Fig. 4A' and C') and a number of TUNEL+ cells were observed (Fig. 2B and B'). In the outer zone, the neuronal loss was less severe and a few large-sized neurons, mainly interneurons, were obvious (Fig. 4A'' and C''). Several apoptotic cells were still observed (Fig. 2B') in this region whereas no TUNEL+ labeling was detected in control rats (data not shown). The neuron number in the outer zone of the MCAO group (Nissl: 18.67 ± 3.51 vs. control 37.67 ± 1.53, $p<0.05$; HE: 18.00 ± 2.00 vs. control 40.67 ± 2.52, $p<0.05$) was lower than that in the controls (Fig. 3B). In the melatonin-treated rats, the ischemic core was limited

to a much smaller size (Fig. 4B and D) and the neuron abundance in the outer zone was significantly higher (Nissl: 29.33 ± 2.00, $p<0.05$; HE: 26.67 ± 2.53, $p<0.05$; Fig. 3B-B'' and D-D''; Fig. 3B) when compared with MCAO rats. The number of the apoptotic cells in the outer zone of the MCAO+MT group (8.67 ± 1.53) was also notably decreased in comparison with the MCAO group (14.00 ± 2.80, $p<0.05$; Fig. 2C and C'; Fig. 3B).

Ischemic Injury of Striatal Projection Neurons and the Protective Effect of Melatonin

Histologically, the striatum consists of a vast majority of medium-sized projection neurons and a small number of interneurons (Durieux et al. 2011). We used the NeuN antibody, which labels brain cell nuclei of all types of neurons in the rat striatum, and found that the expression of NeuN is observed in most neuronal cell types throughout the nervous system, including the striatum of vertebrates according to the previous study (Mullen et al. 1992). The Darpp-32 antibodies were applied to specifically label striatal projection neurons. In accordance with the previous study (Ouimet and Greengard 1990), immunoreactivity for Darpp-32 was mainly present in dendritic spines, dendrites and the perikaryal cytoplasm of the medium-sized spiny projection neurons in the rat caudate-putamen in the present study. The results showed that the projection neurons mainly survived in the outer zone of the infarct instead of the ischemic core. However, the cell count in the outer zone of the MCAO group (10.33 ± 1.53) was still decreased when compared
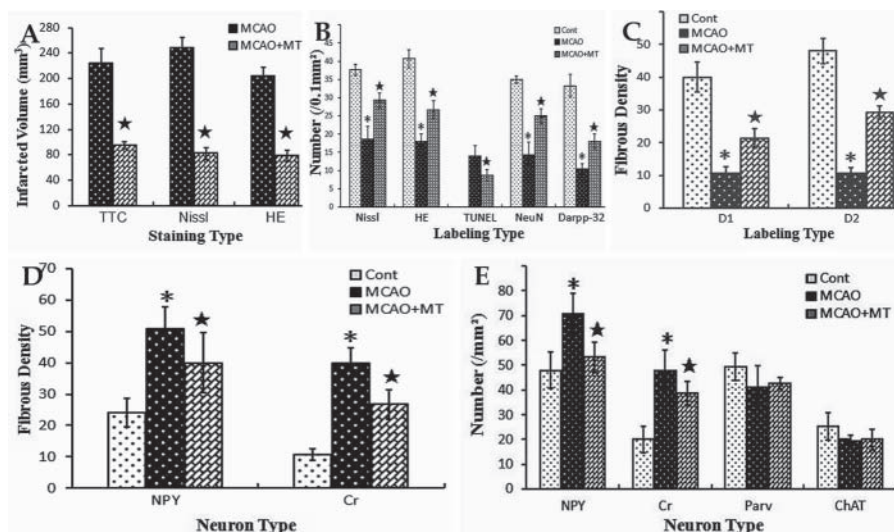
Figure 3. Comparison of the striatal ischemic volume and injury degree of different neuron types among groups. The data shown are a bar graph representation from the data in Fig. 2 and 4–8. Histogram A shows that the infarcted volume of the MCAO+MT group was smaller than that of the MCAO group. Histogram B shows that the neuron number in the outer zone of the infarct was significantly decreased in the MCAO group when compared with controls, but it was notably alleviated in the MCAO+MT group; the number of TUNEL+ cells in the outer zone was lower in the MCAO+MT group than in the MCAO group. Histogram C shows that the densities of D1+ and D2+ fibers in the outer zone were significantly reduced in the MCAO group whereas they were improved in the MCAO+MT group. Histogram D shows that the fiber densities of NPY+ and Cr+ interneurons in the outer zone were significantly elevated in the MCAO group when compared with controls, but they were alleviated in the MCAO+MT group. Histogram E shows that the numbers of NPY+ and Cr+ interneurons in the outer zone were significantly increased in the MCAO group, but the changes of the two interneuron types were weakened in the MCAO+MT group; however, the numbers of both Parv+ and ChAT+ neurons in the outer zone were not significantly different between the MCAO+MT and MCAO groups. *$p<0.05$ MCAO vs. Cont (control, or sham-operated); ★$p<0.05$ MCAO+MT vs. MCAO.

with controls (33.25 ± 3.08, $p<0.05$; Fig. 5E and E'; Fig. 3B). With melatonin treatment, the abundance of the Darpp-32+ neurons in the outer zone was significantly higher in the MCAO+MT group (18.00 ± 2.30, $p<0.05$) than in the MCAO group (Fig. 5F and F'; Fig. 3B). These results were in accordance with the observation from the histochemical Nissl and HE staining (Fig. 4) and immunostaining of NeuN (MCAO 14.33 ± 3.53 vs. control 35.00 ± 1.00, $p<0.05$; MCAO+MT 25.00 ± 4.20 vs. MCAO, $p<0.05$; Fig. 3B).

The striatal projection neurons form two efferent pathways. Dendrites and dendritic spines of the projection neurons in the direct pathway are specifically labeled by antibodies against D1 receptors whereas those in the indirect pathway are labeled by antibodies against D2 receptors (Kreitzer and Berke 2011). The present results showed that both D1+ and D2+ fibers were sparse in the ischemic core of the MCAO group (Fig. 6B, B', E and E') unlike the uniform and dense distribution in the striatum of control rats (Fig. 6A, A', D and D'). The densities of D1+ (10.67 ± 2.08 vs. control 40.00 ± 4.62, $p<0.05$) and D2+ (10.67 ± 1.67 vs. control 48.00 ± 3.80, $p<0.05$) fibers in the outer zone of the MCAO group were evidently lower than those in controls (Fig. 3C). In the melatonin-treated rats, the densities of D1+ (21.33 ± 3.06, $p<0.05$) and D2+ fibers (29.33

± 2.00, $p<0.05$) in the outer zone were significantly higher when compared with those in the MCAO group (Fig. 6C, C', F and F'; Fig. 3C).

Specific Responses of Ischemic Striatal Interneurons and the Effect of Melatonin

Interneurons only account for about 5–10% of all striatal neurons. They are classified into four types—choline acetyltransferase (ChAT)+, parvalbumin (Parv)+, calretinin (Cr)+, and NPY/SS/nNOS+ neurons, which coexpress the peptides neuropeptide Y (NPY) and somatostatin (SS) as well as the enzyme neuronal nitric oxide synthase (nNOS) (Durieux et al. 2011). As shown in Nissl, HE and NeuN staining, yjr large-sized neurons scattered among the projection neurons were mostly interneurons (Fig. 4; Fig. 5). In line with previous studies, the present research showed that the antibody against the calcium binding protein Parv specifically labeled the cytoplasm, including the perikarya and processes of the neostriatal GABAergic Parv+ neurons, which were mainly distributed in the dorsolateral striatum (Cowan et al. 1990; Tepper et al. 2010); the antibody against ChAT labeled the perikarya of the cholinergic neurons in the central nervous system, including the striatum (Oda
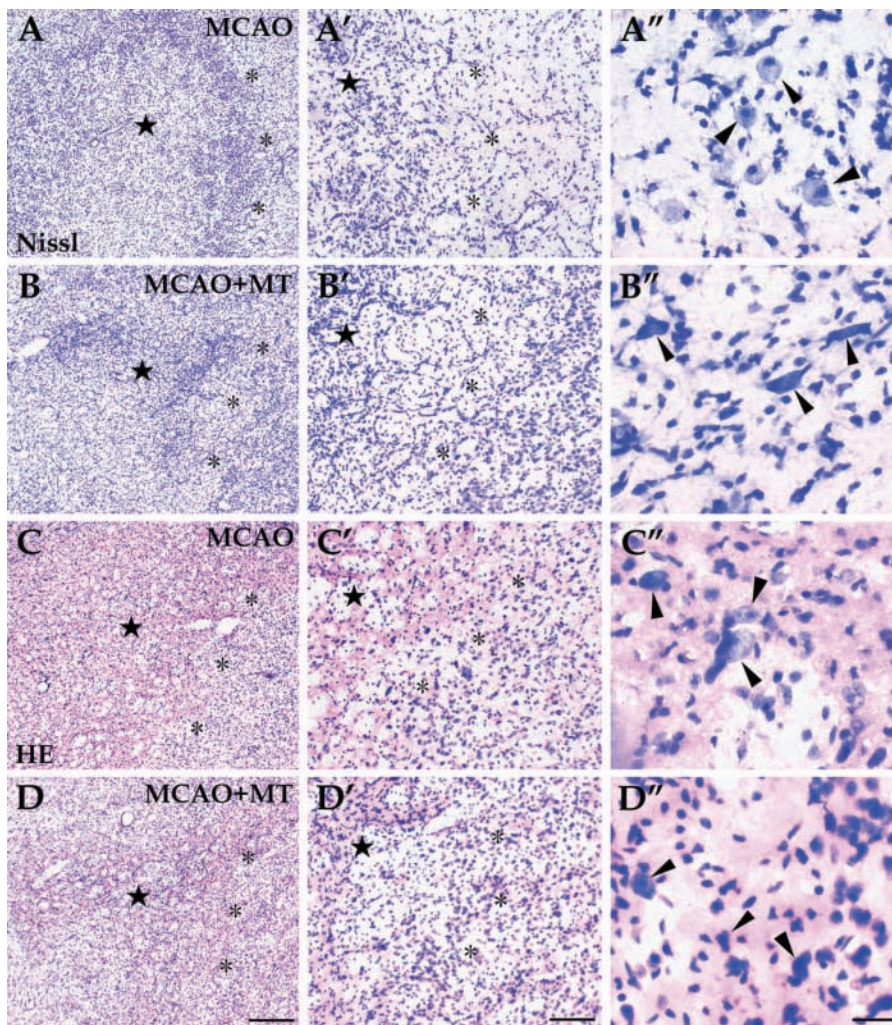
Figure 4. Histological changes in ischemic striatum with melatonin treatment. The infarcted area, located in the dorsolateral striatum, consisted of a dark-stained ischemic core (★) and a pale-stained outer zone (*) surrounding the ischemic core. Both Nissl (image sets A and B) and HE staining (image sets C and D) showed severe neuron loss and infiltration of inflammatory cells in the ischemic core whereas the neuron loss was less severe and a few large-sized neurons survived (arrowheads) in the outer zone. However, in the MCAO+MT group (image sets B and D), the ischemic core appeared smaller and more neurons survived in the outer zone than in the MCAO group (image sets A and C). Scale bars: A–D, 250 μm; A'–D', 100 μm; A"–D", 30 μm.

1999); the staining of NPY included the cell bodies and processes of this striatal neuron type, which were observed throughout the striatum (Riedel et al. 2002); the antibody against the calcium binding protein Cr labeled the somata and fibers of these neostriatal GABAergic neurons, which were mainly distributed in the medial striatum (Mura et al. 2000). Based on the morphological analyses from brain sections in the present study, the somas of Parv+ and ChAT+ interneurons were large-sized (Fig. 8 A-A'' and D-D'') whereas the somas of NPY+ and Cr+ neurons were medium-sized (Fig. 7 A-A'' and D-D'').

Both NPY+ interneurons and Cr+ ones presented similar changes. In contrast to striatal projection neurons, which were notably decreased in cell number within the infarcted area of the MCAO group, the number of these two interneuron types was just slightly decreased in the ischemic core (data not shown) and was even significantly elevated in the outer zone (NPY+ neurons: 70.68 ± 8.32 vs. control 48.00 ± 7.20, $p<0.05$; Cr+ neurons: 48.00 ± 8.00 vs. control

20.00 ± 5.36, $p<0.05$) when compared with controls (Fig. 7B-B'' and E-E''; Fig. 3E). In addition, the densities of NPY+ (50.67 ± 7.05 vs. control 24.00 ± 4.62, $p<0.05$) and Cr+ fibers (40.00 ± 4.62 vs. control 10.67 ± 1.76, $p<0.05$) in the outer zone of the MCAO group were both significantly increased in comparison with controls (Fig. 3D). These dense fibers formed large networks and developed strings of varicosities along the processes (Fig. 7B'' and E''). The phenomenon of hyperplasia of axons in NPY+ and Cr+ neurons were diminished with melatonin treatment as in the MCAO+MT group (Fig. 7C-C'' and F-F''). Quantitative analyses showed that the cell counts and fiber densities of both kinds of interneurons in the MCAO+MT group (NPY+ neurons: 53.32 ± 6.12; Cr+ neurons: 38.68 ± 4.80; NPY+ fibers: 40.00 ± 9.61; Cr+ fibers: 26.67 ± 4.62) were notably lower than those in the MCAO group (all $p<0.05$; Fig. 3D; Fig. 3E).

As for Parv+ and ChAT+ interneurons, a few survived in the ischemic core in the MCAO group. Unlike NPY+ and
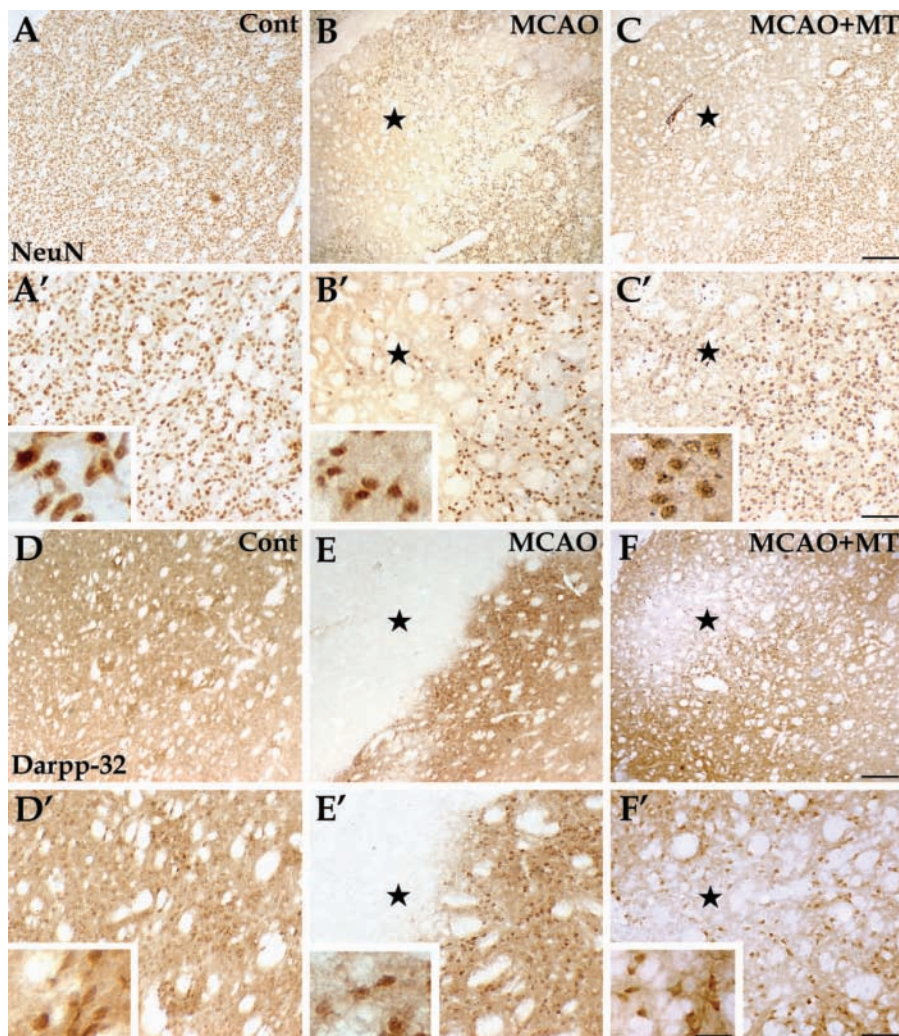
Figure 5. Improvement in the levels of neuronal damage in ischemic striatum with melatonin treatment. Striatal neurons, presented with NeuN labeling (A, A', B, B', C, and C'), were evenly distributed throughout the striatum in the control group (A and A'). In the MCAO group (B and B'), the NeuN+ cells were extremely scarce in the ischemic core (★) and significantly reduced in quantity in the outer zone. In the MCAO+MT group (C and C'), however, the infarcted size was reduced and more NeuN+ cells survived in the outer zone. Similar manifestation was observed in the striatal projection neurons, which were specifically labeled by Darpp-32 (D, D', E, E', F, and F')—the infarcted area was broad with very few labeled cells in the MCAO group (E and E') whereas it was notably improved in the MCAO+MT group (F and F'). Cont is short for control (or sham-operated). Scale bars: A–F, 250 µm; A'–F', 100 µm; small images in A'–F', 30 µm.

Cr+ cells, however, the numbers of these two interneuron types in the outer zone of the infarct (Parv+ neurons: 41.32 ± 8.32 vs. control 49.32 ± 5.60; ChAT+ neurons: 19.48 ± 2.32 vs. control 25.32 ± 5.52) were close to that of the control group (Fig. 8B, B', E and E'). With melatonin treatment, changes in the two interneuron types were similar to that in ischemic rats (Fig. 8C-C'' and F-F''). Statistical analyses did not show a significant difference between the MCAO and MCAO+MT groups (Parv+ neurons: 42.68 ± 2.28; ChAT+ neurons: 20.00 ± 4.00; Fig. 3E).

Discussion

Specific Striatal Impairments Induced by MCAO

Occlusion of the MCA has been widely used to induce ischemic stroke in animals because the MCA mainly supplies the striatum, a major target of injury in cerebrovascular accidents (Block et al. 2005; Bacigaluppi et al. 2010).

Studies have revealed that MCAO results in behavioral deficits and the underlying neuronal damages of the caudate-putamen (Tamura et al. 1981; Marston et al. 1995; Sakai et al. 1996; Mu et al. 2011b). In accordance with these results, the present study confirmed that MCAO rats developed striatum-related dysfunction of locomotion, coordination and cognition. The mammalian striatum has long been implicated in motor behavior, and recent studies indicate a role for the basal ganglia, in particular the dorsal striatum, in learning and memory (Packard and Knowlton 2002; El et al. 2007). As shown in our results, MCAO rats presented with body rigidity and difficulty in initiating movement in the balance beam test and in the grip strength test, and exhibited cognitive and mnemonic deficits, which manifested as an impairment in the acquisition of the stimulus-response (S-R) habit in the Morris water maze task. Yet it is necessary to differentiate the mnemonic dysfunction of the striatum from that of the hippocampus because the hippocampus is a classic, important structure involved
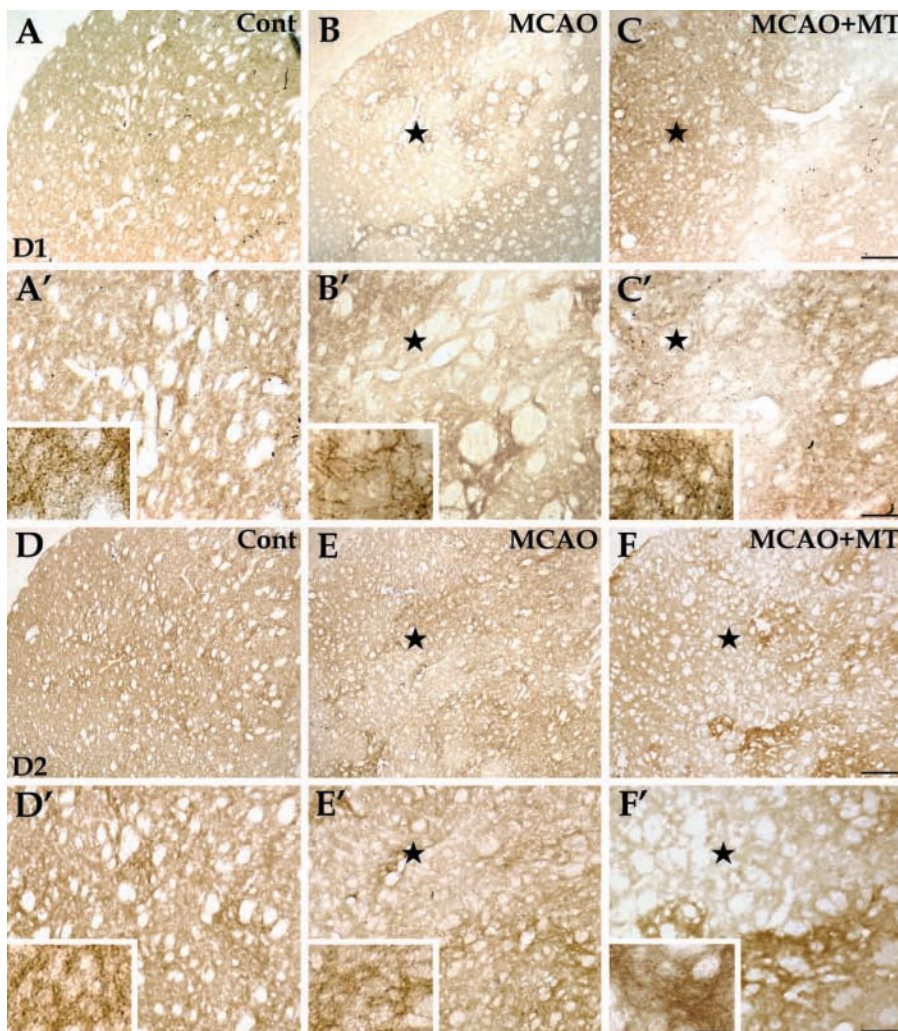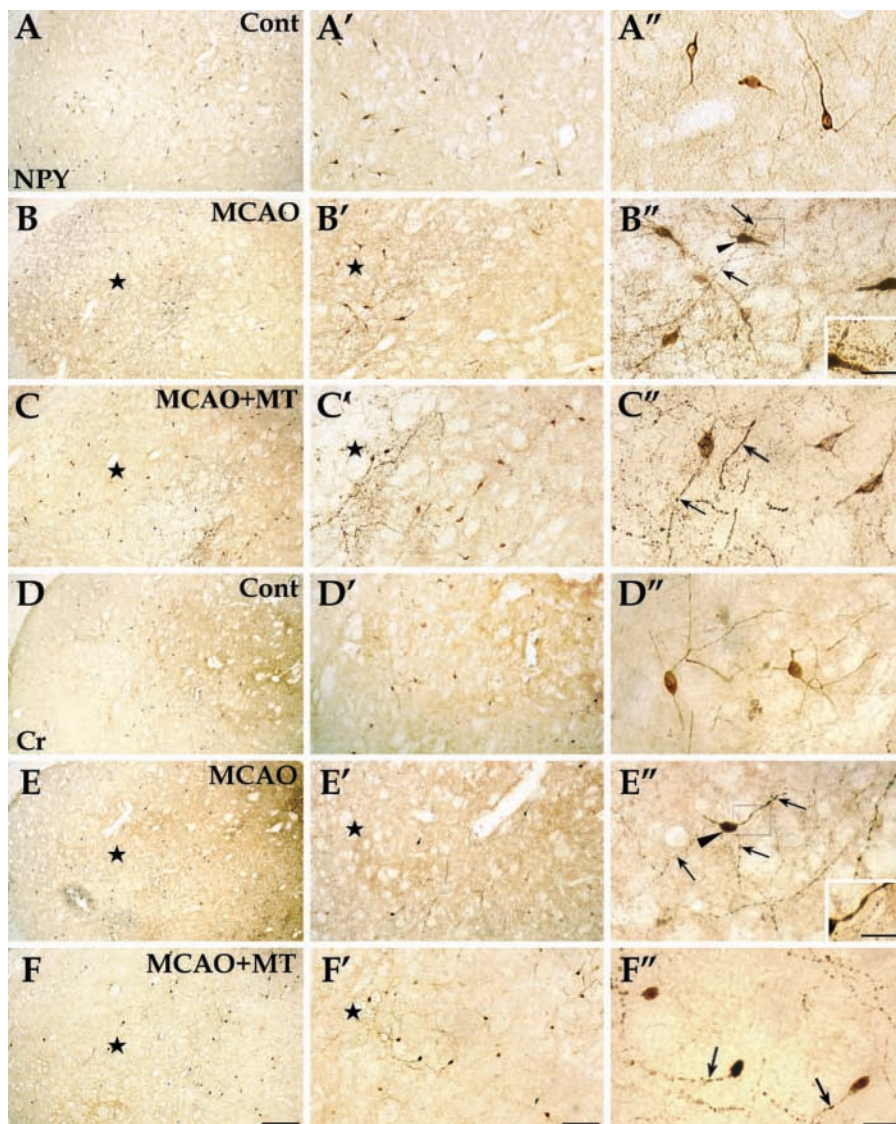
Figure 6. Changes of D1+ and D2+ neurons in ischemic striatum with melatonin treatment. In brain sections with immunolabeling of D1+ neurons (A, A', B, B', C, and C'), the immunolabeled structures, presented as neuropils, were densely and evenly distributed in the striatum of the control group (A and A'). In the MCAO group (B and B'), the D1+ neuropils were nearly absent in the ischemic core (★) but changes of the D1+ neurons in the outer zone of the infarct were less severe. In the MCAO+MT group (C and C'), however, the infarcted size was reduced and D1+ fibers appeared denser in the outer zone. As for immunolabeling of D2+ neurons (D, D', E, E', F, and F'), the immunolabeled neuropils were also densely and evenly distributed in the striatum of the control group (D and D'). The D2+ neuropils were scarce in the ischemic core (★) and those existing in the outer zone were aggregated as mass in the MCAO group (E and E'). In the MCAO+MT group (F and F'), the infarcted size was reduced and the density of D2+ fibers was significantly increased in the outer zone. Cont is short for control (or sham-operated). Scale bars: A–F, 250 µm; A'–F', 100 µm; small images in A'–F', 30 µm.

in cognitive functions and can be injured by direct ischemia or by indirect inflammatory changes resulting from MCAO (Block et al. 2005). The present study applied the S-R habit version of the water maze task to specifically detect impairment of striatal mnemonic function; dysfunction of the hippocampal memorial system did not interfere with the acquisition of the task (Packard and Knowlton 2002). Therefore, this striatal injury model further confirmed that the striatum is critically involved in motor and cognitive functions. It is well known that the striatal GABAergic projection neurons play a pivotal role in motor control of the striatum (Chuhma et al. 2011) whereas the striatal interneurons are mediators of the activities of projection neurons (Berke 2011). Recent research also suggested that striatal GABAergic and cholinergic neurons are implicated in the mnemonic functions of the basal ganglia (Packard and Knowlton 2002). Yet the specific physiological functions and interconnection of these different types of striatal neurons have not been clearly clarified. The severe damage to

the striatal projection neurons in our present findings may imply that this neuron type plays a more critical part in motor and cognitive functions of the striatum than the striatal interneurons.

In line with previous studies, our results demonstrated that the infarcted region of the striatum, where neurons underwent severe injury, apoptosis and loss, exhibited a particular pattern—an ischemic core with severe neuronal loss and an outer zone with milder neuronal damages (Pestalozza et al. 2002; Guadagno et al. 2004). The outer zone of the infarct, also called penumbra, proves to be a crucial region determining the survival or death of neurons; as such, it is regarded as a feasible and effective target for treatment of ischemic stroke (Liu et al. 2010).

Even though neurons were detected surviving in the outer zone, several studies reported that various types of striatal neurons displayed different sensitivity to ischemic insult—projection neurons were rather vulnerable to injury whereas interneurons were relatively resistant (Goto et al.
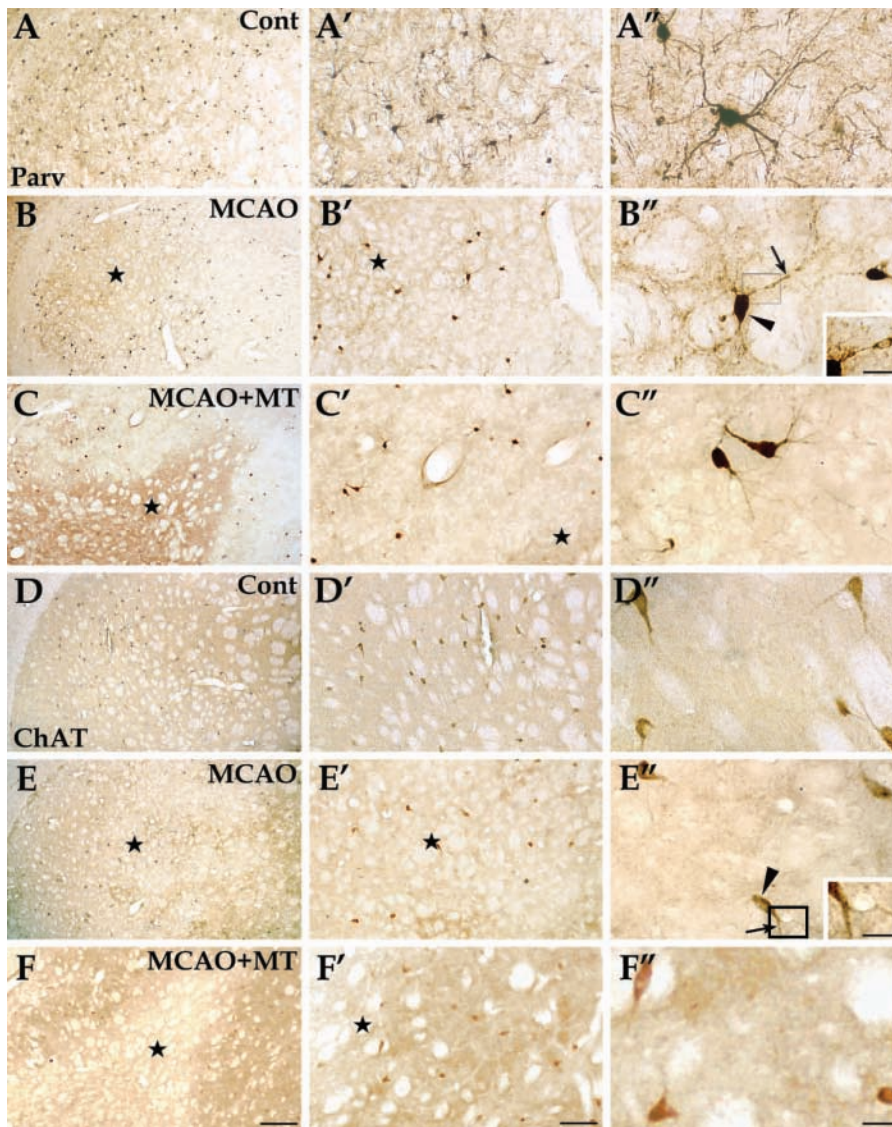
Figure 7. Specific reactions of NPY+ and Cr+ interneurons in ischemic striatum with melatonin treatment. In brain sections with immunolabeling of NPY+ cells (image sets A, B, and C), this interneuron type was evenly distributed in the striatum and their cell bodies and processes were clearly observed in the control group (image set A). In the MCAO group (image set B), the abundance of the NPY+ cells in the ischemic core (★) were slightly reduced; in the outer zone of the infarct a notable hyperplasia of the NPY+ interneurons was observed and they formed large fiber networks and developed varicosities (arrows). In the MCAO+MT group (image set C), however, the infarcted size was reduced and the increase of the cell abundance and fiber density in the outer zone was not as high as that of the MCAO group. In the Cr-labeled striatum sections (image sets D, E, and F), the Cr+ interneurons were mainly distributed in the medial striatum in controls (image set D). The specific reactions of this interneuron were similar to those of the NPY+ cells—the cell number and fiber density with varicosity formation were significantly elevated in outer zone of the infarct of the MCAO group (image set E), but these changes were remitted in the MCAO+MT group (image set F). Arrowheads indicate the neuronal cell bodies. Cont is short for control (or sham-operated). Inserts in B" and E" were magnifications of the areas in the rectangle frame, scale bars: 15 μm. Scale bars: A–F, 250 μm; A'–F', 100 μm; A"–F", 30 μm.

1993; Kokaia et al. 1998; Meade et al. 2000; Larsson et al. 2001). In agreement with several other studies, Darpp-32 immunolabeling in our results showed an extensive reduction in the number of projection neurons in the infarcted region, including the outer zone (Chesselet et al. 1990; Mallard et al. 1995). The mechanisms of energy impairment, oxidative stress, excitotoxicity, and inflammation may underlie this pathophysiology of projection neurons (Dirnagl et al. 1999). The vulnerability of striatal projection neurons was also observed in HD models induced by the mitochondrial toxin 3NP or the excitotoxin QA (Figueredo-Cardenas et al. 1998; Brouillet et al. 2005). Furthermore, projection neurons in the indirect pathway were found to be affected earlier and more severely than

neurons in the direct pathway during the pathological progress of HD (Han et al. 2010). Nevertheless, the two different subtypes of projection neurons seemed to have similar susceptibility to ischemic damage, as was shown in the present data.

The resistance of different striatal interneuron types to ischemic insult has been reported lately (Meade et al. 2000). The present study also revealed that most of the interneurons that survived in the ischemic core and the numbers of Parv+ neurons and ChAT+ neurons were not significantly decreased in the outer zone of the infarct. Their resistance to injury may be due to their low density of glutamate receptors, facility in Ca^{2+} sequestering, or ability to scavenge free radicals (Dolga et al. 2011). Intriguingly, the present study further recorded

Figure 8. Specific reactions of Parv+ and ChAT+ interneurons in ischemic striatum with melatonin treatment. The Parv+ interneurons (image sets A, B, and C), normally with large cell bodies and a great many processes, were mainly distributed in the dorsolateral striatum in the control group (image set A). In the MCAO group (image set B), only a few Parv+ interneurons were observed in the ischemic core (★) but the cell count in the outer zone of the infarct seemed close to controls. The changes appeared similar in the MCAO+MT group (image set C). In the ChAT-labeled striatum sections (image sets D, E, and F), the ChAT+ interneurons which possessed large cell bodies and a few neural processes were evenly scattered throughout the striatum in controls (image set D). The cell abundance in the ishemic core appeared lower than controls both in the MCAO group (image set E) and in the MCAO+MT group (image set F) but not in the outer zone in both groups. The arrowhead indicates the neuronal cell body; arrow indicates the process. Cont is short for control (or sham-operated). Inserts in B” and E” were magnifications of the areas in the rectangle frame, scale bars: 15 μm. Scale bars: A–F, 250 μm; A’–F’, 100 μm; A”–F”, 30 μm.

that NPY+ interneurons and Cr+ ones within the outer zone showed resistance with an increase in cell number and morphological changes including hyperplasia of processes and the formation of varicosities along the processes. Though very few studies have reported on the hyperplasia and morphological changes to striatal interneurons after ischemic damage, our observation was supported by Figueredo-Cardenas et al. (1998) who found that neonatal hypoxia/ischemia resulted in the neurogenesis of Cr+ striatal interneurons in rats. In addition, our previous studies on HD model induced by 3NP proved that the survival of the Cr+ and NPY+ interneurons in the transition zone was accompanied by an increase in labeling of their processes and varicosities (Mu et al. 2011b; Mu et al. 2011c). The significance of this is still controversial. On one hand, it may be regarded as a response to compensate for the great loss of projection neurons; on the other hand, it may be a protective reaction in that the protein calretinin (Cr) plays an important role in the maintenance of intracellular Ca^{2+} homeostasis and its presence in some neurons may protect them against the massive Ca^{2+} entry that may result from overstimulation of glutamate receptors (Cicchetti et al. 2000).

It should be noted that accurate measurements of neuron numbers and fiber densities of different striatal neuron types may be compromised by several technical shortcomings in the present study: (1) the cerebral ischemic model was induced by permanent MCAO which may presumably interfere with perfusion and fixation, and would in turn affect the antibody staining. This may have led to an underestimation in counting, but the procedure of postfixation in the present

study should have helped correct for this and the cerebral ischemia–reperfusion model, which is also widely used to study brain ischemia, might probably avoid this technical shortcoming; (2) brain sections of 50 μm thickness in the present study should contain 2 to 6 layers of neurons depending on the diameters of neuronal somata (Tepper et al. 2010), and the technical limitations made it hard to determine whether the tissue was stained through the full thickness of the section; thus the exact neuron numbers and fiber densities might have been underestimated in all animals, including the controls; (3) neuron measurements were determined by profile counts, which might have not reflected the accurate changes in cell abundance and fiber densities, especially in the condition of ischemia. This possibly resulted in changes of cell diameters in response to inflammation and hypoxia, so the stereologically unbiased methods may solve this problem by providing more precise data of neuron numbers (Covey and Oorschot 2007).

Neuroprotective Effects of Melatonin on Ischemic Injury

Melatonin is considered to be a highly potent antioxidant and scavenger of free radicals (Reiter et al. 1996). It has been reported that melatonin has been tested as a neuroprotective agent in a variety of neurodegenerative diseases (Reiter et al. 1999; Srinivasan et al. 2005). Lately, experiments on melatonin have extended to include treatment for cerebral ischemia. An earlier study found that melatonin reduced cerebral edema formation, the early symptom of ischemia, so as to reduce subsequent chronic neural damage in stroke patients (Kondoh et al. 2002). Now, increasing evidence shows that melatonin can reduce neurophysiological deficits, infarct volume, the degree of neural edema, and neuron and glial loss (Reiter et al. 2005). In addition, its neuroprotective effects are similar whether melatonin is given before or after ischemic onset (Kilic et al. 2004b). The present study also demonstrated that melatonin ameliorated sensorimotor and cognitive dysfunction; the improvement in neuronal damage and morphological transformation underscore these behavioral changes. Our results showed that the loss of projection neurons and axonal hyperplasia in NPY+ and Cr+ interneurons were relieved by melatonin treatment whereas the Parv+ and ChAT+ interneurons appeared less affected, which suggests that different types of striatal neurons have different physiological functions. Yet an adequate description of the specific functions of different striatal neurons is difficult given the prescribed limits of the present study.

Our data further confirmed that melatonin treatment protected the striatum against ischemic damage as demonstrated by the reductions in the infarcted area, neuronal apoptosis and loss. The underlying mechanisms have been extensively studied and the outstanding ability of melatonin to reduce oxidative stress is most emphasized (Pei et al. 2002b). In addition to its antioxidant actions, research has also revealed that melatonin exerts its protective effects by improving mitochondrial function and interfering with both proapoptotic cell signaling and synthesis of inflammatory cytokines (Cervantes et al. 2008). Furthermore, recent evidence demonstrates that the activation of MT2 melatonin receptor in the hippocampal CA1 region may be involved in the neuroprotective effect of melatonin after ischemic injury (Lee et al. 2010). This suggests that the melatonin receptor pathway may also play a role in the protective effects of melatonin in the ischemic striatum because the expression of melatonin receptor mRNA has been detected in the striatum (Uz et al. 2003).

At present, there were hardly any studies reporting the effects of melatonin on different types of striatal neurons after ischemic damage. Our previous research on 3NP-induced HD model indicated that loss of both striatal projection neurons and interneurons were relieved by melatonin treatment and that the morphological changes of interneurons were also ameliorated (Mu et al. 2011b). The present study revealed a similar phenomenon in the striatal ischemic model that melatonin inhibited hyperplasia and morphological transformation of both Cr+ interneurons and NPY+ ones. Yet the underlying mechanisms have not been clarified. Presumably, the overall protective effects of melatonin might play a major role in alleviating neuronal hyperplasia. In addition, several studies have demonstrated that melatonin might work as an inhibitor of nitric oxide synthase (NOS) to reduce oxidative stress (Cervantes et al. 2008; Camacho et al. 2012) and such an effect of melatonin might suppress hyperplasia of NPY+ interneurons that coexpress nNOS (Kawaguchi 1993; Nair et al. 2011). In conclusion, our results demonstrate that melatonin exerts neuroprotective effects in ischemic striatal neurons, which indicates the great potential of melatonin to be applied in the clinic as a neuroprotective agent for ischemic brain injury.

Declaration of Conflicting Interests

Funding

References

Avendano C, Roda JM, Carceller F, Diez-Tejedor E. 1995. Morphometric study of focal cerebral ischemia in rats: a stereological evaluation. Brain Res. 673:83–92.

Bacigaluppi M, Comi G, Hermann DM. 2010. Animal models of ischemic stroke. Part two: modeling cerebral ischemia. Open Neurol J. 4:34–38.

Berke JD. 2011. Functional properties of striatal fast-spiking interneurons. Front Syst Neurosci. 5:45.

Block F, Dihne M, Loos M. 2005. Inflammation in areas of remote changes following focal brain lesion. Prog Neurobiol. 75:342–365.

Brouillet E, Jacquard C, Bizat N, Blum D. 2005. 3-nitropropionic acid: a mitochondrial toxin to uncover physiopathological mechanisms underlying striatal degeneration in Huntington's disease. J Neurochem. 95:1521–1540.

Camacho ME, Carrion MD, Lopez-Cara LC, Entrena A, Gallo MA, Espinosa A, Escames G, Acuna-Castroviejo D. 2012. Melatonin synthetic analogs as nitric oxide synthase inhibitors. Mini Rev Med Chem. 12:600–617.

Carmichael ST. 2005. Rodent models of focal stroke: size, mechanism, and purpose. NeuroRx. 2:396–409.

Cervantes M, Morali G, Letechipia-Vallejo G. 2008. Melatonin and ischemia-reperfusion injury of the brain. J Pineal Res. 45:1–7.

Chesselet MF, Gonzales C, Lin CS, Polsky K, Jin BK. 1990. Ischemic damage in the striatum of adult gerbils: relative sparing of somatostatinergic and cholinergic interneurons contrasts with loss of efferent neurons. Exp Neurol. 110:209–218.

Chuhma N, Tanaka KF, Hen R, Rayport S. 2011. Functional connectome of the striatal medium spiny neuron. J Neurosci. 31:1183–1192.

Cicchetti F, Gould PV, Parent A. 1996. Sparing of striatal neurons coexpressing calretinin and substance P (NK1) receptor in Huntington's disease. Brain Res. 730:232–237.

Cicchetti F, Prensa L, Wu Y, Parent A. 2000. Chemical anatomy of striatal interneurons in normal individuals and in patients with Huntington's disease. Brain Res Brain Res Rev. 34:80–101.

Covey MV, Oorschot DE. 2007. Effect of hypothermic post-treatment on hypoxic-ischemic striatal injury, and normal striatal development, in neonatal rats: a stereological study. Pediatr Res. 62:646–651.

Cowan RL, Wilson CJ, Emson PC, Heizmann CW. 1990. Parvalbumin-containing GABAergic interneurons in the rat neostriatum. J Comp Neurol. 302:197–205.

Dirnagl U, Iadecola C, Moskowitz MA. 1999. Pathobiology of ischaemic stroke: an integrated view. Trends Neurosci. 22:391–397.

Dolga AM, Terpolilli N, Kepura F, Nijholt IM, Knaus HG, D'Orsi B, Prehn JH, Eisel UL, Plant T, Plesnila N, Culmsee C. 2011. KCa2 channels activation prevents [Ca2+]i deregulation and reduces neuronal death following glutamate toxicity and cerebral ischemia. Cell Death Dis. 2:e147.

Donnan GA, Fisher M, Macleod M, Davis SM. 2008. Stroke. Lancet. 371:1612–1623.

Durieux PF, Schiffmann SN, de Kerchove DA. 2011. Targeting neuronal populations of the striatum. Front Neuroanat. 5:40.

El MN, Cheruel F, Faure A, Conde F. 2007. Learning and memory dissociation in rats with lesions to the subthalamic nucleus or to the dorsal striatum. Neuroscience. 147:906–918.

Figueredo-Cardenas G, Harris CL, Anderson KD, Reiner A. 1998. Relative resistance of striatal neurons containing calbindin or parvalbumin to quinolinic acid-mediated excitotoxicity compared to other striatal neuron types. Exp Neurol. 149:356–372.

Goto S, Nagahiro S, Korematsu K, Ushio Y. 1993. Striatonigral involvement following transient focal cerebral ischemia in the rats: an immunohistochemical study on a reversible ischemia model. Acta Neuropathol. 85:515–520.

Guadagno JV, Warburton EA, Aigbirhio FI, Smielewski P, Fryer TD, Harding S, Price CJ, Gillard JH, Carpenter TA, Baron JC. 2004. Does the acute diffusion-weighted imaging lesion represent penumbra as well as core? A combined quantitative PET/MRI voxel-based study. J Cereb Blood Flow Metab. 24:1249–1254.

Han I, You Y, Kordower JH, Brady ST, Morfini GA. 2010. Differential vulnerability of neurons in Huntington's disease: the role of cell type-specific features. J Neurochem. 113:1073–1091.

Hyakkoku K, Nakajima Y, Izuta H, Shimazawa M, Yamamoto T, Shibata N, Hara H. 2009. Thalidomide protects against ischemic neuronal damage induced by focal cerebral ischemia in mice. Neuroscience. 159:760–769.

Kawaguchi Y. 1993. Physiological, morphological, and histochemical characterization of three classes of interneurons in rat neostriatum. J Neurosci. 13:4908–4923.

Kilic E, Kilic U, Reiter RJ, Bassetti CL, Hermann DM. 2004a. Prophylactic use of melatonin protects against focal cerebral ischemia in mice: role of endothelin converting enzyme-1. J Pineal Res. 37:247–251.

Kilic E, Kilic U, Yulug B, Hermann DM, Reiter RJ. 2004b. Melatonin reduces disseminate neuronal death after mild focal ischemia in mice via inhibition of caspase-3 and is suitable as an add-on treatment to tissue-plasminogen activator. J Pineal Res. 36:171–176.

Koh PO. 2008. Melatonin attenuates the cerebral ischemic injury via the MEK/ERK/p90RSK/bad signaling cascade. J Vet Med Sci. 70:1219–1223.

Koh PO. 2012. Melatonin attenuates decrease of protein phosphatase 2A subunit B in ischemic brain injury. J Pineal Res. 52:57–61.

Kokaia Z, Andsberg G, Martinez-Serrano A, Lindvall O. 1998. Focal cerebral ischemia in rats induces expression of P75 neurotrophin receptor in resistant striatal cholinergic neurons. Neuroscience. 84:1113–1125.

Kondoh T, Uneyama H, Nishino H, Torii K. 2002. Melatonin reduces cerebral edema formation caused by transient forebrain ischemia in rats. Life Sci. 72:583–590.

Kreitzer AC, Berke JD. 2011. Investigating striatal function through cell-type-specific manipulations. Neuroscience. 198:19–26.

Larsson E, Lindvall O, Kokaia Z. 2001. Stereological assessment of vulnerability of immunocytochemically identified striatal and hippocampal neurons after global cerebral ischemia in rats. Brain Res. 913:117–132.

Lee CH, Yoo KY, Choi JH, Park OK, Hwang IK, Kwon YG, Kim YM, Won MH. 2010. Melatonin's protective action against ischemic neuronal damage is associated with up-regulation of the MT2 melatonin receptor. J Neurosci Res. 88:2630–2640.

Liu F, Schafer DP, McCullough LD. 2009. TTC, fluoro-Jade B and NeuN staining confirm evolving phases of infarction induced by middle cerebral artery occlusion. J Neurosci Methods. 179:1–8.

Liu S, Levine SR, Winn HR. 2010. Targeting ischemic penumbra: part I—from pathophysiology to therapeutic strategy. J Exp Stroke Transl Med. 3:47–55.

Maldonado MD, Murillo-Cabezas F, Terron MP, Flores LJ, Tan DX, Manchester LC, Reiter RJ. 2007. The potential of melatonin in reducing morbidity-mortality after craniocerebral trauma. J Pineal Res. 42:1–11.

Mallard EC, Waldvogel HJ, Williams CE, Faull RL, Gluckman PD. 1995. Repeated asphyxia causes loss of striatal projection neurons in the fetal sheep brain. Neuroscience. 65:827–836.

Marston HM, Faber ES, Crawford JH, Butcher SP, Sharkey J. 1995. Behavioural assessment of endothelin-1 induced middle cerebral artery occlusion in the rat. NeuroReport. 6:1067–1071.

Matsumori Y, Hong SM, Fan Y, Kayama T, Hsu CY, Weinstein PR, Liu J. 2006. Enriched environment and spatial learning enhance hippocampal neurogenesis and salvages ischemic penumbra after focal cerebral ischemia. Neurobiol Dis. 22:187–198.

Meade CA, Figueredo-Cardenas G, Fusco F, Nowak TJ, Pulsinelli WA, Reiner A. 2000. Transient global ischemia in rats yields striatal projection neuron and interneuron loss resembling that in Huntington's disease. Exp Neurol. 166:307–323.

Mu S, OuYang L, Liu B, Qu H, Zhu Y, Li K, Lei W. 2011a. Relationship between inflammatory reaction and ischemic injury of caudate-putamen in rats: inflammatory reaction and brain ischemia. Anat Sci Int. 86:86–97.

Mu S, OuYang L, Liu B, Zhu Y, Li K, Zhan M, Liu Z, Jia Y, Lei W. 2011b. Protective effect of melatonin on 3-NP induced striatal interneuron injury in rats. Neurochem Int. 59:224–234.

Mu S, OuYang L, Liu B, Zhu Y, Li K, Zhan M, Liu Z, Jia Y, Lei W, Reiner A. 2011c. Preferential interneuron survival in the transition zone of 3-NP-induced striatal injury in rats. J Neurosci Res. 89:744–754.

Mullen RJ, Buck CR, Smith AM. 1992. NeuN, a neuronal specific nuclear protein in vertebrates. Development. 116:201–211.

Mura A, Feldon J, Mintz M. 2000. The expression of the calcium binding protein calretinin in the rat striatum: effects of dopamine depletion and L-DOPA treatment. Exp Neurol. 164:322–332.

Nair SM, Rahman RM, Clarkson AN, Sutherland BA, Taurin S, Sammut IA, Appleton I. 2011. Melatonin treatment following stroke induction modulates L-arginine metabolism. J Pineal Res. 51:313–323.

Nishino H, Koide K, Aihara N, Kumazaki M, Sakurai T, Nagai H. 1993. Striatal grafts in the ischemic striatum improve pallidal GABA release and passive avoidance. Brain Res Bull. 32:517–520.

Oda Y. 1999. Choline acetyltransferase: the structure, distribution and pathologic changes in the central nervous system. Pathol Int. 49:921–937.

Ouimet CC, Greengard P. 1990. Distribution of DARPP-32 in the basal ganglia: an electron microscopic study. J Neurocytol. 19:39–52.

Packard MG, Knowlton BJ. 2002. Learning and memory functions of the Basal Ganglia. Annu Rev Neurosci. 25:563–593.

Pei Z, Ho HT, Cheung RT. 2002a. Pre-treatment with melatonin reduces volume of cerebral infarction in a permanent middle cerebral artery occlusion stroke model in the rat. Neurosci Lett. 318:141–144.

Pei Z, Pang SF, Cheung RT. 2002b. Pretreatment with melatonin reduces volume of cerebral infarction in a rat middle cerebral artery occlusion stroke model. J Pineal Res. 32:168–172.

Pestalozza IF, Di Legge S, Calabresi M, Lenzi GL. 2002. Ischaemic penumbra: highlights. Clin Exp Hypertens. 24:517–529.

Quay WB. 1989. Changes with darkness in regional brain 5-hydroxytryptamine and 5-hydroxyindole acetic acid: local differences with pinealectomy, sham surgery, and melatonin. Neurochem Res. 14:957–961.

Reiter RJ, Cabrera J, Sainz RM, Mayo JC, Manchester LC, Tan DX. 1999. Melatonin as a pharmacological agent against neuronal loss in experimental models of Huntington's disease, Alzheimer's disease and parkinsonism. Ann N Y Acad Sci. 890:471–485.

Reiter RJ, Oh CS, Fujimori O. 1996. Melatonin Its intracellular and genomic actions. Trends Endocrinol Metab. 7:22–27.

Reiter RJ, Tan DX, Leon J, Kilic U, Kilic E. 2005. When melatonin gets on your nerves: its beneficial actions in experimental models of stroke. Exp Biol Med (Maywood). 230:104–117.

Riedel A, Hartig W, Seeger G, Gartner U, Brauer K, Arendt T. 2002. Principles of rat subcortical forebrain organization: a study using histological techniques and multiple fluorescence labeling. J Chem Neuroanat. 23:75–104.

Sakai N, Yanai K, Ryu JH, Nagasawa H, Hasegawa T, Sasaki T, Kogure K, Watanabe T. 1996. Behavioral studies on rats with transient cerebral ischemia induced by occlusion of the middle cerebral artery. Behav Brain Res. 77:181–188.

Shear DA, Dong J, Gundy CD, Haik-Creguer KL, Dunbar GL. 1998. Comparison of intrastriatal injections of quinolinic acid and 3-nitropropionic acid for use in animal models of Huntington's disease. Prog Neuropsychopharmacol Biol Psychiatry. 22:1217–1240.

Srinivasan V, Pandi-Perumal SR, Maestroni GJ, Esquifino AI, Hardeland R, Cardinali DP. 2005. Role of melatonin in neurodegenerative diseases. Neurotox Res. 7:293–318.

Tamura A, Graham DI, McCulloch J, Teasdale GM. 1981. Focal cerebral ischaemia in the rat: 1. Description of technique and early neuropathological consequences following middle cerebral artery occlusion. J Cereb Blood Flow Metab. 1:53–60.

Tan DX, Manchester LC, Terron MP, Flores LJ, Reiter RJ. 2007. One molecule, many derivatives: a never-ending interaction of melatonin with reactive oxygen and nitrogen species? J Pineal Res. 42:28–42.

Tepper JM, Tecuapetla F, Koos T, Ibanez-Sandoval O. 2010. Heterogeneity and diversity of striatal GABAergic interneurons. Front Neuroanat. 4:150.

Uz T, Akhisaroglu M, Ahmed R, Manev H. 2003. The pineal gland is critical for circadian Period1 expression in the striatum and for circadian cocaine sensitization in mice. Neuropsychopharmacology. 28:2117–2123.

Voogd J, Feirabend HKP. 1981. Methods in neurobiology. Vol 2. New York: Elsevier.

Vorhees CV, Williams MT. 2006. Morris water maze: procedures for assessing spatial and related forms of learning and memory. Nat Protoc. 1:848–858.

Yamori Y, Horie R, Handa H, Sato M, Fukase M. 1976. Pathogenetic similarity of strokes in stroke-prone spontaneously hypertensive rats and humans. Stroke. 7:46–53.

Yang YF, Chen Z, Hu SL, Hu J, Li B, Li JT, Wei LJ, Qian ZM, Lin JK, Feng H, Zhu G. 2011. Interleukin-1 receptor associated kinases-1/4 inhibition protects against acute hypoxia/ischemia-induced neuronal injury in vivo and in vitro. Neuroscience. 196:25–34.

Yang Z, You Y, Levison SW. 2008. Neonatal hypoxic/ischemic brain injury induces production of calretinin-expressing interneurons in the striatum. J Comp Neurol. 511:19–33.